The Underwater Venting of Methanol Vapour

Cédric De Boom, Aris Twerda, Alex W. Vredeveldt & Martijn Hoogeland
Netherlands Organisation for Applied Scientific Research TNO, Anna van Buerenplein 1, Den Haag 2595 DA, The Netherlands

ABSTRACT: Sailing on methanol supports the decarbonisation of shipping. Venting under water is a solution to avoid dangerous zones, normally created by venting toxic methanol above deck. An Eulerian based Computational Fluid Dynamics (CFD) model and a simple integral model are used to predict the methanol concentration above the waterline after underwater venting of methanol vapour. Both models are successfully validated against experimental data from a methane release at the bottom of a water basin. The CFD model showed superiority over the integral model.

The numerical models are applied on a mixture of methanol and nitrogen being vented during bunkering. The gas dissolution depends strongly on the bubble diameter and venting depth. The CFD model shows in the most critical case the gas dissolution being sufficient and no methanol vapour reaches the deck of the ship. The underwater venting of methanol-nitrogen vapour proves to be a safe alternative compared to venting above deck.

1 INTRODUCTION

To meet the shipping industry's emissions reduction goals, it is imperative to explore and adopt alternative marine fuels. Methanol (or methyl alcohol) is expected to play a large role in the future of decarbonization of shipping. However, current regulations limit the attractiveness of methanol as marine fuel for some ship types due to the need of a (high) venting mast to avoid a large unusable space around a venting point. Hazardous area zones are needed around fuel tank vapour outlets due to the flammability and toxicity of methanol vapour. To avoid risk for humans, the outlets shall be positioned such that the distance to crewed areas is sufficiently large. Consequently, for smaller ships, the outlets need a large mast to create these distances which is impractical feature, also in view of air draught, or deck spaces are closed off for daily operations.

Usually, a critical concentration at 30 minutes exposure of 6000ppm (0.6 vol%) is used which corresponds to the Immediate Danger to Life and Health of methanol (IDLH) (National Institute for Occupational Safety and Health, 1994).

An alternative venting arrangement is proposed by creating an underwater vent. Methanol dissolves well in water and is considered not toxic for aquatic life. This novel solution has not been incorporated in ship design due to a lack of available supporting calculations and experiments. In this paper numerical supporting information is provided.

Very little research has been conducted on the underwater venting of vapour. Nevertheless, information can be obtained from similar scenarios, such as gas release of subsea pipeline ruptures such as performed in the Rotvoll experiment (Ross, 2009, Ahmed et al, 2021). From this research different zones were chosen to represent the governing physics. After a subsea gas release, the bubbles will rise through these different zones in the water column. These zones (flow establishment, established flow, surface and atmosphere zone) are depicted in Figure 1. The dominating physics will change in each zone. An important driving force is the buoyancy which depends on the density ratio of the released gas and the displaced liquid. Other mechanisms governing the bubble plume are drag, turbulence and gas dissolution.

This paper investigates the venting of the fuel tank vapour below the waterline instead of above deck to be able to limit/ eliminate measures such as large vent musts or unusable deck space. Numerical models are applied to compute the concentration on deck. These are described in Section 2. The cases are detailed in Section 3 and their results respectively in Section 4. Finally, conclusions will be presented in Section 5.

2 NUMERICAL INVESTIGATION

2.1 *Integral method*

Integral models assume that plume velocities and gas fractions can be represented by certain mathematical profiles, mostly Gaussian profiles. These models are called ”integral” because the governing set of equations is based on an integral over the width of the profiles (Olsen and Skjetne, 2015). Integral models use a constant angle to describe the widening of the plume. See Figure 1. The applied integral model is based on the widely used so-called Friedl model (Friedl and Fanneløp, 2000) and the model built by Loes and Fanneløp, (1989) for the plume above the water surface. The Friedl model is a theoretical model which mainly focuses on the fountain, which is the elevation of the water surface due to a subsea gas release.

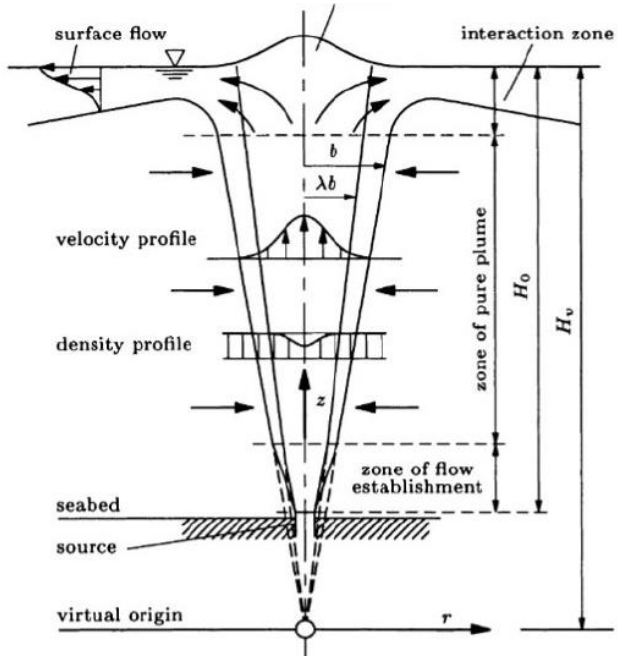

Figure 1 Sketch of time-averaged bubble plume used in the integral method taken from Friedl and Fanneløp (2000)

2.2 *Computational Fluid Dynamics*

In CFD models the transport equations describing the conservation of mass, momentum, energy, and species are solved. The CFD simulation is set up in ANSYS-Fluent (version 22.2). Buoyancy and gravity are included in the model and the density is calculated using the incompressible ideal gas model. The Reynolds Averaged Navier Stokes (RANS) model k-ε is used as turbulence model.

Two types of models can solve particle transport (gas through water), namely Euler–Euler and Euler–Lagrange models.

In the Euler-Euler model, the particles are considered as a continuum phase, just like the water. The particles are a virtual fluid described by momentum transport equations similar to the Navier-Stokes equations. In the Euler-Lagrange model, the particles are followed individually and not as a fluid. The description for the movement of a particle is described by Newton’s second law. The Lagrangian model (in comparison to the Eulerian model) can calculate the particle size distribution with a lower computational cost (Wojciech and Adamczyk, 2014). The Eulerian-Lagrangian Discrete Phase Model (DPM) is applied for the simulation of the underwater gas release. This model will track a parcel of bubbles in the Lagrangian frame and will monitor the change in properties in the Eulerian frame. The drag force of the bubble is taken from Xia et.al. (2001) which according to Cloete et al (2009) represents the behaviour of a bubble plume. The ambient fluid is treated as a continuum by solving the Navier-Stokes equations. The surface (interface between seawater and air) is tracked by a scheme in the Volume of Fluid (VOF) model. This method uses explicit discretization and represents the interface between fluids using a piecewise-linear approach.

2.2.1 *Dissolution*

Because methanol can dissolve easily in water, this effect must be incorporated in the model. The mass transfer rate through the surface of the bubble with diameter (d_b) can be calculated as follows (Skjetne and Olsen, 2012):

$$\dot{m} = \pi d_b^2 k_i \rho_l n_i^{sol} \frac{M_i}{M_l} \quad (1)$$

Where ρ_l is the liquid density, M is the molar weight and n is the solubility of the compound in the surrounding liquid. The concentration of the dissolved gas in the surrounding liquid is assumed to be negligible. k is the mass transfer coefficient and the subscript i represents a certain chemical compound (methane or methanol). For the mass transfer coefficient, the following Sherwood relation as function of Reynolds (Re) and Schmidt (Sc) number is used.

$$Sh = \frac{k}{D/d_b} = 2 + 0.552 Re^{1/2} Sc^{1/3} \quad (2)$$

With D the molecular diffusivity. The solubility of gases in water can be calculated by the well-known Henry’s law (Herman, 2017).

2.2.2 *Bubble size*

The drag coefficient is dependent on the bubble size. In addition, the gas dissolution or mass transfer from gas bubbles to the surrounding liquid is dependent on the bubble surface area. A correct bubble size distribution is therefore required to achieve accurate simulation results. The instantaneous local mean bubble diameter (d_b) is described by the balance between the local time derivative of the local bubble diameter and an equilibrium term which accounts for breakup and coalescence (Cloete et al, 2009):

$$\frac{\partial d_b}{\partial t} = \frac{(d_b^{eq} - d_b)}{\tau_{rel}} \qquad (3)$$

τ_{rel} is the relaxation time, which is the time needed for the bubble to return to the bubble equilibrium diameter. The relaxation time is determined by the speed of breakup or coalescence and is modelled as a characteristic timescale for both processes according to (Pan, 2014) and (Laux and Johansen, 1999). A mathematical expression for the equilibrium diameter (d_b^{eq}), derived from experiments in a stirred tank, is given by Calderbank (1958).

$$d_b^{eq} = C_1 \phi_b^{0.5} \left(\frac{\sigma}{\rho}\right)^{0.5} \left(\frac{\mu_b}{\mu}\right)^{0.25} \epsilon^{-0.4} + C_2 \qquad (4)$$

Where ϵ is the dissipation of turbulent kinetic energy, μ_b is the viscosity of the bubble phase and σ is the surface tension between bubbles and the surrounding fluid. ϕ_b is the bubble void fraction which is the volume fraction that bubbles occupy in the water. This bubble fraction is calculated by the gas concentration (in kg/m3) divided by the gas density which is computed by means of the ideal gas law. C_1 is a dimensionless constant and is equal to 4.0 and C_2 is the minimum bubble size and is equal to 0.1mm (Pan, 2014).

3 CASES

3.1 *Rotvoll Experiment*

The numerical models, described in Section 2, should have a solid basis. Therefore, first a model validation should be performed where the measured gas concentrations from an underwater gas release are compared to the predicted concentrations from the numerical model. This model will be afterwards adapted to the methanol venting experiment. In the past, multiple experiments of subsea gas releases have been carried out. In 1997 a series of experiments were conducted in a 7-meter-deep freshwater basin with a surface area of 6x9m at Statoil's (now Equinor) Research center in Trondheim. A mixture of helium and air was used, to obtain the same density as natural gas, to monitor the gas concentration above the surface. To measure gas concentration and velocities below the surface, air was injected. The gas was released at different flow rates from a circular opening of 0.17m diameter at 6.9m from the water surface. The plume characteristics were captured by a high-speed camera. Table 1 shows the parameters and results of the experiment.

Table 1 Parameters and results of Rotvoll experiment (Sjoen et al. 1997)

Flow rates (m3/s) / (Nm3/s)	Mass flow rates (kg/s) methane/air	Inlet Velocity (m/s)	Rise time (s)	Initial fountain height (m)	Maximum fountain height (m)
0.05/0.083	0.03/0.10	2.2	6.0	-	-
0.1/0.17	0.06/0.21	4.4	4.8	0.3	0.65
0.45/0.75	0.3/0.92	19.6	3.1	0.45	1.24

3.1.1 *CFD case set-up*

For the CFD a polyhedral mesh was mode with local grid refinement in the cone and near the air-water surface as can be seen in Figure 2. All settings mentioned in Section 2.2 are applied.

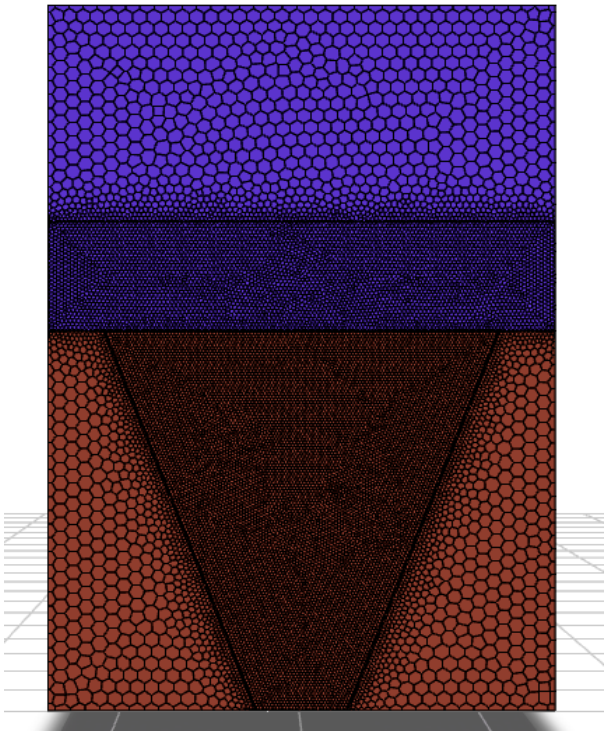

Figure 2 Polyhedral mesh with conical regional refinements

Boundary conditions are set to be able to solve momentum and continuity equations. Except for the top surface of the mesh, the boundary type is designated as ”wall” with a no-slip condition. Since bubbles will reflect upon hitting a wall, it is important to position these surfaces in such a way that they do not affect the results. The initial bubble size is constant and taken from the equilibrium diameter formula given in Equation 4. A typical result of the flow of the particles is depicted in Figure 3, where the colouring is done with the residence time of the particle.

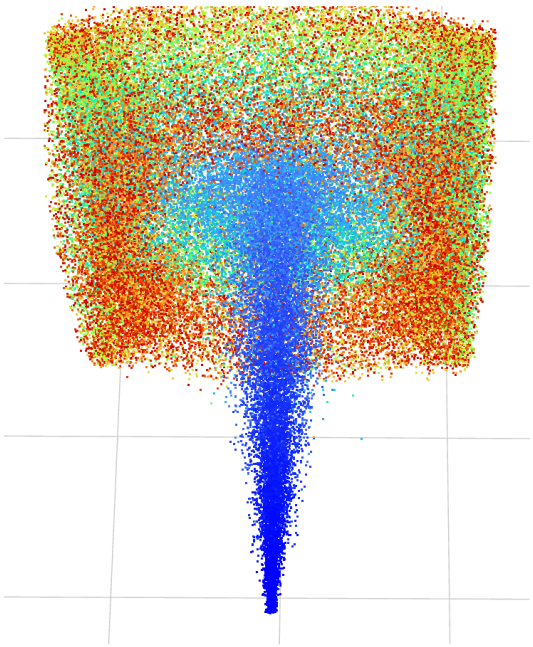

Figure 3 Particle tracks of Rotvoll experiment (0.20 kg/s release rate), seen from below.

3.2 *Methanol venting*

For the methanol venting a full-scale setup was used. The geometry simulated is shown in Figure 4. Also, here a polyhedral mesh was applied. A careful selection of boundary conditions helps to ensure that the simulation results are physically meaningful. The boundaries (surfaces) of the geometry (see Figure 4) are described here. The surfaces of the ship and the bunker barge are set as walls. The interface between the water and air surface is an internal boundary type. The particles can leave the domain at the bottom surface of the geometry, below the (keel of the) bunker barge, 2m to the aft or front of the release point, above the deck of the bunker barge and above the deck of the ship. These surfaces below the waterline are walls but with the DPM escape setting and the surfaces above the waterline are pressure outlets.

A pressure relief valve (PRV) is used to build up pressure in the bunker tank to overcome the hydrostatic back pressure before venting. For relief pressure 14 kPa is used and the closing pressure is 9 kPa.

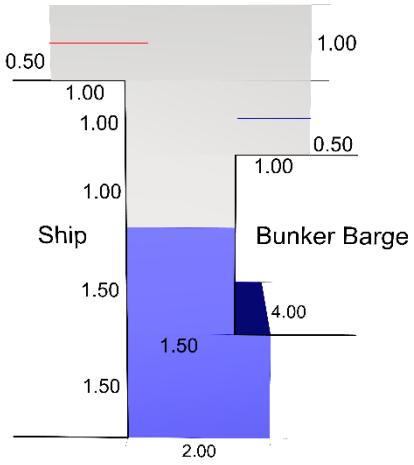

Figure 4 Geometry full scale methanol-nitrogen venting (blue: water, grey: air)

These values are characteristic for a PRV on a vessel. The mass release rate also depends on the volume of the bunker tank. As the pressure will decrease when the valve opens, the mass flow will decrease. This can be seen in Figure 5 where the released mass flow rate is plotted versus time without closing. Note that the closing pressure of the valve is reached after approx. 18s. After this time the pressure rises again until the opening pressure is reached, and the release process is repeated.

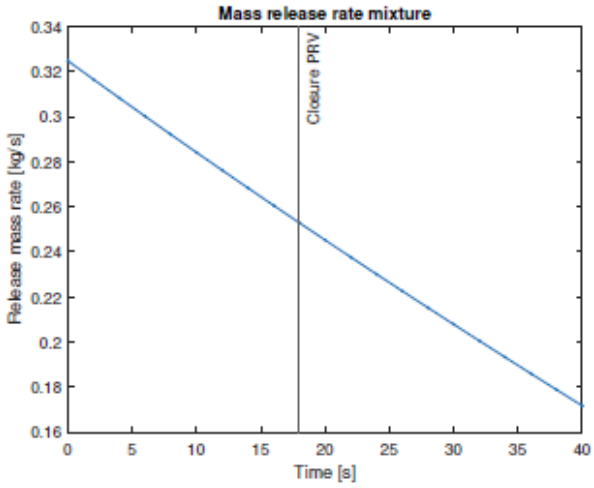

Figure 5 Released mass in function of time without closing. The valve.

4 RESULTS AND DISCUSSION

4.1 *Rotvoll Experiment*

Figure 6 shows the velocity at the centerline in function of the height, where 0 is the bottom of the basin and 7m is at the water surface. At low heights there is a large difference between the CFD model and the integral model. This is due to zero initial velocity, of the liquid, which is not taken into account in the integral model. After the release, the velocity increases due to the buoyancy and afterwards it decreases due to the drag force. The integral model shows a larger discrepancy near the surface due to the radial movement of the water.

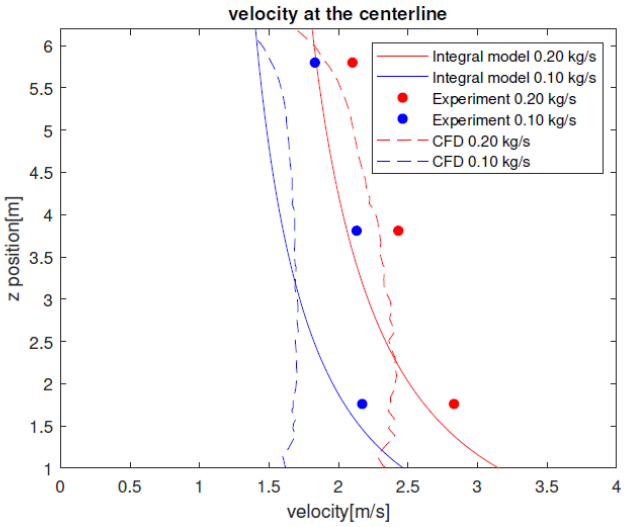

Figure 6 Comparison velocity at centerline between the Rotvoll experiment, integral model and CFD

This can be explained due to lacking surface interaction in the model. When the gas reaches the surface there is an increasing number of turbulent eddies, leading to an erroneous velocity profile close to the surface. Both the CFD and the integral deviate more from the experiments in the case with a release rate of 0.10 kg/s. This is mainly due to the use of parameters which are fitted to the 0.20 kg/s release rate case. The underestimation of the velocity in the CFD model is probably due to incorrect initial bubble size. When a larger bubble is injected, the buoyancy is larger and consequently also the velocity.

Figure 7 shows the concentration of methane 1m above the water surface. In the top figure the original implementation is shown with and without the solubility considered (time averaged over 180s). The highest concentration is not measured directly above the release point (at the center of the plume) but at 1m away from the center. This is just outside of the fountain region (where the water is pushed upwards). There seems to be an overestimation of gas dissolution of bubbles further away from the centerline.

Due to the radial flow below the waterline these bubbles have a longer residence time in the water and therefore more time to dissolve. A reduction factor in the mass transfer from the gas to the water could be used to avoid this discrepancy. An alternative computation method to take a lower gas dissolution into account is used and can be seen in bottom plot of Figure 7. This matches the experimental results better.

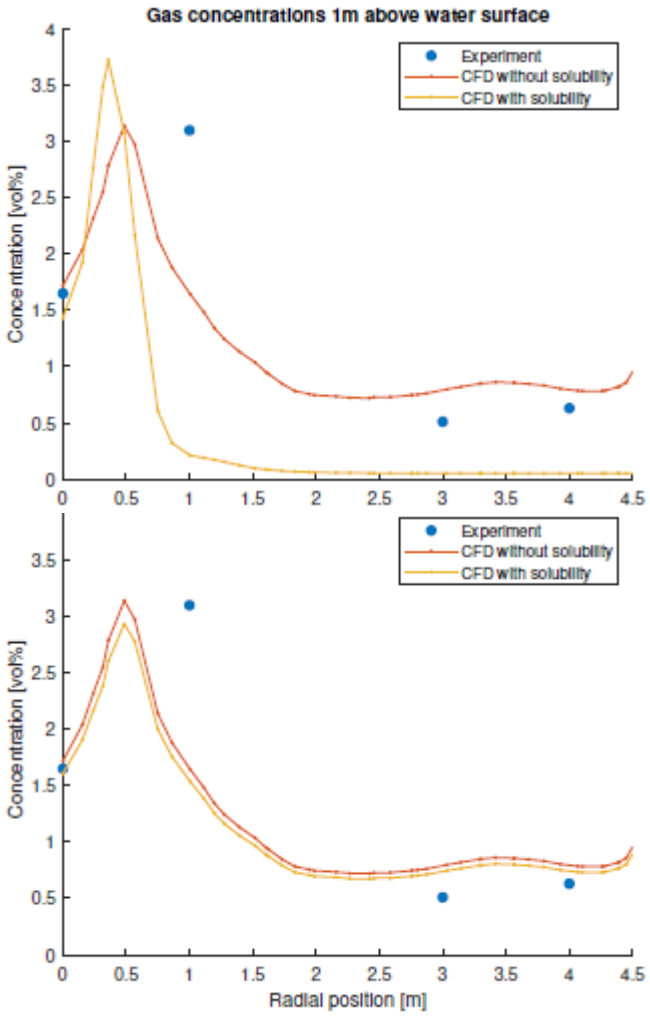

Figure 7 Comparison methane concentrations between the experiment and CFD for 1m above the water surface. Top without alteration below with alteration of the mass transfer for the dissolution.

4.2 *Methanol venting*

In the simulations of the Rotvoll experiment, detailed in the previous section, it was shown that the gas dissolution close to the surface was overestimated by CFD see Figure 7). Therefore, the mass transfer in Equation 2 is multiplied with 0.5 to be on the conservative side. As the closing pressure of the pressure relief valve is 9 kPa, the maximal venting depth should be 0.9m to overcome the hydrostatic pressure.

Figure 8 shows the particle tracks of methanol vapour at the end of a gas injection. The injection is chosen to have a duration of 18s with a release rate of 0.30 kg/s which is conservative compared to Figure 4. The released vapour consists out of 100% methanol, which is an overestimation except when the bunker tank is almost completely filled. The with an initial bubble size diameter 0.002m, calculated with Equation 4, there is a complete dissolution of the methanol in the surrounding water. Due to this gas dissolution, the methanol is not able to rise to the surface. If nitrogen would be present it will remain in the bubble and will reach the water surface. As previously stated, the saturation of methanol in the surrounding water is not taken into account. If this were the case, more methanol would be able to rise. However, due to external currents and waves, there will be always a supply of new/ under saturated water leading to an increase of mass transfer of methanol vapour to the water. To quantify that is very difficult. Figure 8 only shows methanol. If the released vapour would consist of a mixture of methanol and nitrogen, there will still be nitrogen vapour above the water surface. Nitrogen has a low solubility.

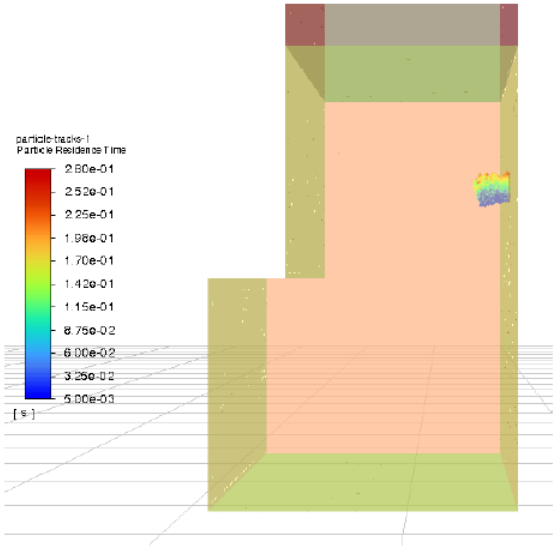

Figure 8 Methanol particle tracks for the full-scale setup from venting at 0.9m depth.

4.2.1 *Bubble size*

Due to the shallow injection depth, the bubbles have very limited time to reach the equilibrium diameter. Figure 9 shows the methanol particle tracks if the departure bubble size diameter would be equal to the diameter of the release opening (0.08m). This is most likely to represent the reality, as in the jetting regime the departure bubble size will lay close to the orifice diameter. In this case, methanol vapour can rise above the water surface at a release depth of 0.5m.

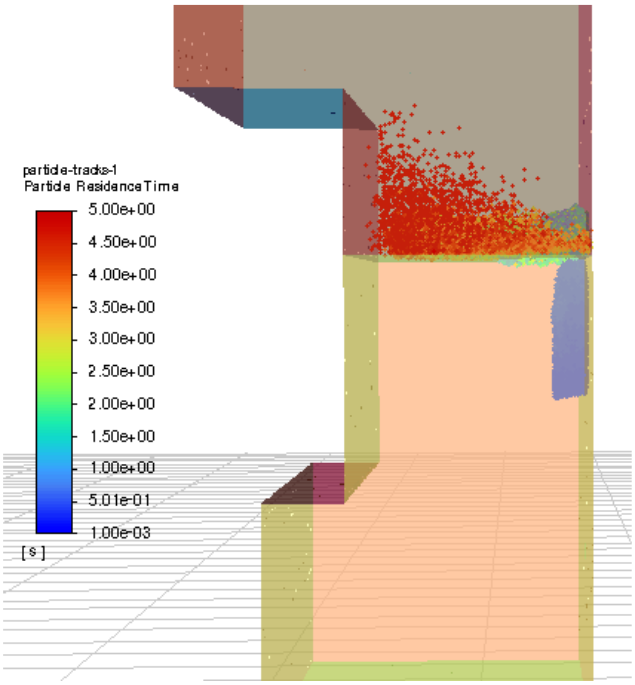

Figure 9 Methanol particle tracks for the full-scale setup (initial bubble size: 0.08m) from venting at 0.9m depth

As an indication, the methanol peak concentration at 0.25m above the water surface is 800ppm. Higher above the water surface, the concentration decreases rapidly and at 0.5m above the water surface only sporadic a methanol particle is found.

4.2.2 *Depth of 0.5m*

Vessels with a smaller draught will vent the methanol at a smaller distance from the waterline (venting depth). The smaller the venting depth, the lower the residence time of methanol in the water leading to a lower gas dissolution rate. Figure 10 shows the result at the end of the venting at 0.5m below the waterline (with an initial bubble size equal to the opening diameter of 0.08m). Even at this lower venting depth no methanol vapour can reach the deck of the barge (or ship). The application of a reduction factor (of 0.5) has little influence due to the short residence time of the methanol vapour in the water. In Figure 11 the methanol concentration at 0.5m above the waterline is depicted. The highest methanol concentration is found close to halfway the bunker barge and the ship. The concentrations are well below the IDLH of 6000ppm.

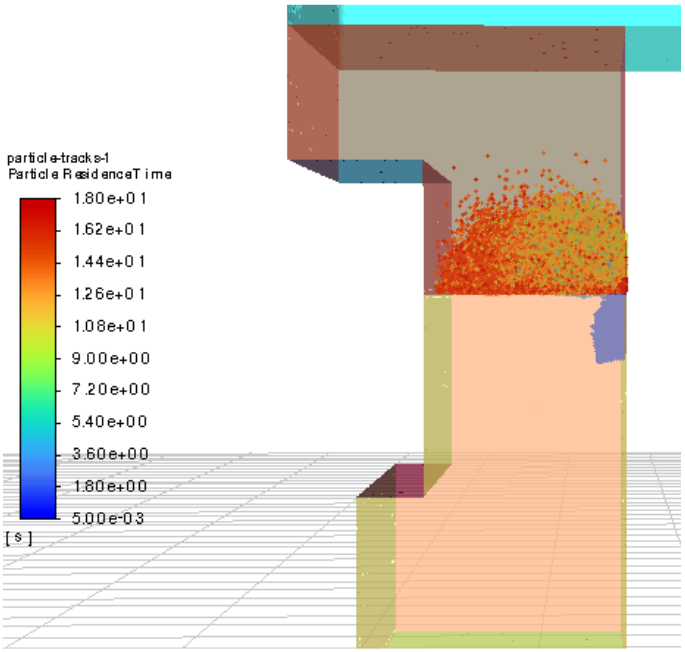

Figure 10 Methanol particle tracks for the full-scale setup (initial bubble size: 0.08m) from venting at 0.5m depth

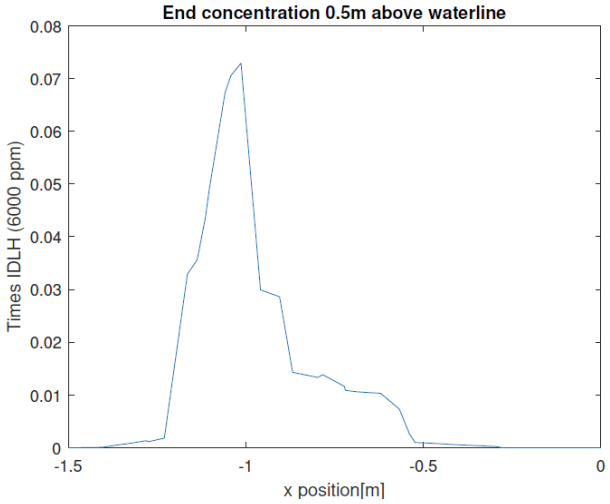

Figure 11 Methanol concentration at 0.5m above the waterline from the venting at 0.5m (x=0: ship, x=-1.5: barge)

5 CONCLUSIONS

The validity of the integral model and CFD model have been tested against an experiment (carried out in 1997) where Helium/ air mixture is injected in a water tank. Results indicated that both models performed reasonably well in predicting velocity and void fraction measurements below the waterline. However, the integral model was found to be less reliable in predicting gas concentrations above the waterline due to several limitations.

The model's lack of consideration for solubility, coupled with the difficulty in estimating coefficients, restricted its general applicability. In contrast, the CFD model's predictions were in good agreement with the gas measurements obtained in the experiment. Although the CFD model over-predicted gas dissolution, this was accounted for by introducing a mass reduction factor. Further investigation in this mass reduction factor or solubility model is required. Looking at the full-scale model the methanol concentration above the waterline is strongly dependent on the gas release rate, venting depth, and the initial bubble size of the released gas. When the initial bubble size is small (e.g., 1cm), the methanol vapour will quickly dissolve after the release. For larger bubble sizes, the venting depth plays an important role. In the most conservative case (8cm initial bubble size and venting depth of 0.5m), the methanol does not fully dissolve in the water, but no methanol vapour is found above 0.5mm above the waterline. Further research to the relation of the orifice diameter (diameter of sea outlet for gas release) and initial bubble diameter will be needed.

The comparison between the methanol concentration on deck due to venting above the waterline, as dictated by the IEC-code, and the methanol concentration on deck due to venting below the waterline, as predicted by the CFD model, has yielded some interesting results. A better validation of the CFD model with methanol would be a recommendation for further research to determine the effect of some model parameters. Furthermore, environmental conditions like wind, water movements, temperature differences are not included and will have an impact on the surfacing plume. These factors might influence the results, but generally will increase the dissolution of methanol in water.

Based on the model assumptions taken, this investigation shows that venting below the waterline has potential to be a valid option to prevent any or strongly reduce methanol vapour on deck. This could be a technique to reduce or even eliminate any potential hazards resulting from toxic or explosive methanol vapour. Hence, it can be stated that venting below the waterline could be used to significantly decrease the hazardous areas and safety distances on deck. This reduction in hazardous areas and safety distances can also result in improved operational efficiency, as it allows for greater flexibility in the placement and operation of equipment and machinery on board the vessel.

ACKNOWLEDGEMENTS

This work was performed within the MENENS project, a consortium of 21 partners (companies and knowledge institutes) covering the entire Dutch maritime sector, sponsored by RVO (Rijksdienst voor Ondernemend Nederland).

REFERENCES

Adamczyk, W. P. et al. 2014. Comparison of the standard Euler–Euler and hybrid Euler–Lagrange approaches for modeling particle transport in a pilot-scale circulating fluidized bed. In: Particuology 15.

Calderbank, P.H. 1958. Physical Rate Processes in Industrial Fermentation, Part I. In: Trans. Inst. Chem. Engrs. (London) 36, p. 443.

Cloete, S., Olsen, J. E & Skjetne. P. 2009. CFD modeling of plume and free surface behavior resulting from a sub-sea gas release. In: Applied Ocean Research 31.3, pp. 220–225.

Ellethy, A. M. et al. 2021. Modelling and Assessment of Accidental Gas Release from Damaged Subsea Pipelines. In: International Journal of Environmental Science and Development 12.6, pp. 162–168

Friedl, M. J. & Fanneløp, T. K. 2000. Bubble plumes and their interaction with the water surface. In: Applied Ocean Research 22.2, pp. 119–128

Herman, S. 2017. Chapter 18 - Fragrance. In: Cosmetic Science and Technology. Ed. by Kazutami Sakamoto et al. Amsterdam: Elsevier

Laux, H. & Johansen, S.T. 1999. A CFD analysis of the air entrainment rate due to a plunging steel jet combining mathematical models for dispersed and separated multiphase flows. In: Proceedings of the Annual TMS Meeting on Fluid Flow Phenomena in Metal Processing, San Diego

Loes, M. & Fanneløp, T. K. 1989. Concentration Measurements Above an Underwater Release of Natural Gas. In: SPE Drilling Engineering 4.02, pp. 171–178

National Institute for Occupational Safety and Health. 1994. Methyl alcohol: Immediately dangerous to life or health concentrations.

Olsen, J. E. & Skjetne. P. 2015. Current understanding of subsea gas release: A review. In: The Canadian Journal of Chemical Engineering 94.2, pp. 209–219

Pan, Q. 2014. Modelling of turbulent flows with strong dispersed phase-continuous fluid interactions. PhD Thesis NTNU.

Ross, S. L., 2009. Assessing Risk and Modeling a Sudden Gas Release Due to Gas Pipeline Ruptures. SINTEF and Wellflow Dynamics.

Sjoen, K., Engebresten, T., Northug, T. & Fanneløp, T. K. 1997. Surface Flow and GasDispersion from a Subsea Release of Natural Gas. In: Proceedings of the 7th International Offshore & Polar Engineering Conference. International Society of Offshore & Polar Eng

Skjetne, P. & Olsen, J. E. 2012. A parcel based modelling concept for studying subsea gas release and the effect of gas dissolution. In: Progress in Computational Fluid Dynamics, An International Journal 12.2/3, p. 187.

Xia, J.L., Ahokainen, T. & Holappa, L. 2001. Analysis of flows in a ladle with gas-stirred melt". In: Scandinavian Journal of Metallurgy 30.2 (Apr. 2001), pp. 69–76.